

Beamforming with Cube Microphone Arrays Via Kronecker Product Decompositions

Xuehan Wang , Jacob Benesty , Jingdong Chen , *Fellow, IEEE*, Gongping Huang ,
and Israel Cohen , *Fellow, IEEE*

Abstract—Microphone arrays combined with beamforming have been widely used to solve many important acoustic problems in a wide range of applications. Much effort has been devoted in the literature to microphone array beamforming, among which the Kronecker product beamforming method developed recently has demonstrated some interesting properties. Generally, this method decomposes the global beamforming filter into a Kronecker product of a number of sub-beamforming filters, each of which corresponds to a virtual subarray and can be designed individually. This decomposition not only reduces significantly the number of beamforming coefficients, but also can be explored to improve the robustness and flexibility of beamforming. This paper extends Kronecker product beamforming from two-dimensional arrays into three-dimensional cube arrays. We consider two decompositions, i.e., fully and partially separable ones. The former decomposes the entire array into three linear subarrays while the latter decomposes the entire array into a linear subarray and a planar one. Then, for each case, we derive the Kronecker product maximum white noise gain beamformer, the Kronecker product approximate maximum directivity factor (DF) beamformer, the Kronecker product null-steering beamformer, and the Kronecker product iterative maximum DF beamformer. Simulation results demonstrate the properties and advantages of the proposed beamformers.

Index Terms—Microphone arrays, cube arrays, three-dimensional arrays, fixed beamforming, Kronecker product, maximum white noise gain beamformer, maximum directivity factor beamformer.

I. INTRODUCTION

MICROPHONE arrays equipped with beamforming techniques are widely employed in various applications for the extraction of desired speech signals in noisy environments.

Manuscript received February 28, 2021; accepted May 4, 2021. Date of publication May 12, 2021; date of current version May 28, 2021. This work was supported in part by the National Key Research and Development Program of China under Grant 2018AAA0102200, by the Key Program of National Science Foundation of China (NSFC) under Grant 61831019, and by the Pazy Research Foundation and the ISF-NSFC joint research program under Grant 2514/17. The associate editor coordinating the review of this manuscript and approving it for publication was Dr. Andy W H Khong. (*Corresponding author: Jingdong Chen.*)

Xuehan Wang and Jingdong Chen are with the Center of Intelligent Acoustics and Immersive Communications, Northwestern Polytechnical University, Xi'an 710072, China (e-mail: wangxuehan.123@mail.nwpu.edu.cn; jingdongchen@ieee.org).

Jacob Benesty is with the INRS-EMT, University of Quebec, Montreal, QC H5A 1K6, Canada (e-mail: benesty@emt.inrs.ca).

Gongping Huang and Israel Cohen are with the Faculty of Electrical and Computer Engineering, Technion-Israel Institute of Technology, Haifa 3200003, Israel (e-mail: gongpinghuang@gmail.com; icohen@ee.technion.ac.il).

Digital Object Identifier 10.1109/TASLP.2021.3079816

Over the last few decades, many beamforming methods have been developed [1]–[10]; the typical ones include the delay-and-sum beamformer, the superdirective beamformer [11]–[16], and differential beamformers [17]–[22], to name but a few.

Conventional beamforming methods generally design the filter directly based on the use of the array outputs [23], [24]. However, this direct method may not fully take advantage of the array geometry to reduce the number of effective beamforming coefficients for performance optimization (in terms of robustness, interference/noise suppression, and computational cost). This could be problematic if the number of microphones in the array is relatively large. For instance, some beamformers involve a coefficient matrix inversion. As the number of microphones increases, the dimension of this matrix to be inverted becomes very large [25], [26]. Then the problem of ill conditioning becomes inevitable, leading to serious beamforming performance degradation in the presence of uncertainties.

Recently, Kronecker product beamforming has been proposed, which offers great promising properties in terms of computational efficiency, robustness, and flexibility [27]–[35]. Generally, this method decomposes the global beamforming filter into a Kronecker product of two or more sub-beamforming filters, each corresponds to a virtual subarray, which can be designed individually. With this decomposition, the number of coefficients that need to be determined or optimized is reduced significantly as compared to the original, global beamforming filter. Matrices involved in each sub-beamformer are also much smaller in dimension, so robustness is easier to achieve. Moreover, one can choose different methods in the design of the different sub-beamformers. As the global beamformer is the Kronecker product of the sub-beamformers, this multistage design offers much flexibility to achieve compromises between conflicted array performance measures [27].

However, existing works on Kronecker product beamforming mainly focus on one-dimensional or two-dimensional arrays, which generally lack flexibility in designing beamformers to enhance signals with sources distributed in the three-dimensional space. In our recent study [30], we applied this principle to a three-dimensional array and presented a method to design Kronecker product beamformers that can achieve a high value of the directivity factor (DF) with a given level of the white noise gain (WNG). In this paper, we study the problem of fixed beamforming with a three-dimensional cube array by using Kronecker product decompositions. We consider two types of array decompositions, i.e., fully and partially separable ones.

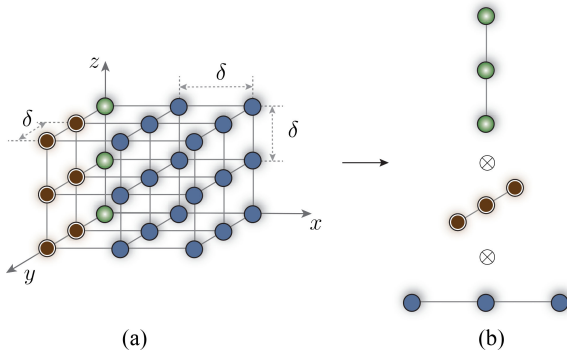


Fig. 1. Illustration of the Kronecker product decomposition of a cube array into three uniform linear subarrays: (a) the cube array and (b) the decomposed linear subarrays.

For the fully separable one, we decompose the entire array into the Kronecker product of three linear subarrays, each along one dimension of the array. For the partially separable one, we decompose the entire array into the Kronecker product of a rectangular subarray and an orthogonal linear subarray. Then, in each case, we deduce a number of fixed sub-beamforming filters, including the maximum WNG (MWNG) and the maximum DF (MDF) ones. Using the Kronecker product formulation, the WNG and DF can be flexibly compromised by combining these optimal sub-beamforming filters. Theoretically, we prove that the Kronecker product maximum WNG beamformers in both cases are equivalent to the conventional global maximum WNG beamformer. We also deduce the Kronecker product null-steering beamformer and the Kronecker product iterative maximum DF beamformer that can maximize the global DF.

The remainder of this paper is organized as follows. In Section II, we present the signal model and problem formulation. In Section III, we expose some conventional fixed beamforming methods as well as some important performance measures. In Sections IV and V, we derive fixed Kronecker product beamformers for the fully and partially separable cases. Simulation results are presented in Section VI to demonstrate the properties of the proposed Kronecker product beamformers. Finally, some conclusions are drawn in Section VII.

II. SIGNAL MODEL AND PROBLEM FORMULATION

The three-dimensional (3D) array considered in this paper is a cube one, which consists of M^3 (with $M \geq 2$) omnidirectional microphones, as shown in Fig. 1(a). This cube array is composed of M parallel square planar uniform arrays with M^2 elements each and the interelement spacing along any axis of the Cartesian coordinate system is equal to δ .

Assume that a farfield source signal (plane wave) propagates from the azimuth angle, φ ($0 \leq \varphi \leq 2\pi$), and elevation (or polar angle), θ ($0 \leq \theta \leq \pi$), in an anechoic acoustic environment at the speed of sound, i.e., $c = 340$ m/s, and impinges on the above described 3D array. Then, the entries of the steering vector, $\mathbf{d}(\omega, \varphi, \theta)$ of length M^3 , are

$$e^{j\frac{\omega\delta}{c}\mathbf{a}^T\mathbf{p}_{ijk}}, \quad i, j, k = 1, 2, \dots, M, \quad (1)$$

where j is the imaginary unit, $\omega = 2\pi f$ is the angular frequency, $f > 0$ is the temporal frequency,

$$\mathbf{a} = [\sin\theta \cos\varphi \sin\theta \sin\varphi \cos\theta]^T, \quad (2)$$

the superscript T is the transpose operator, and \mathbf{p}_{ijk} , $i, j, k = 1, 2, \dots, M$ are the positions (with unit of length) of the M^3 sensors, with $\mathbf{p}_{111} = [0 \ 0 \ 0]^T$. It can be verified that $\mathbf{d}(\omega, \varphi, \theta)$ can be decomposed as

$$\mathbf{d}(\omega, \varphi, \theta) = \mathbf{d}_1(\omega, \varphi, \theta) \otimes \mathbf{d}_2(\omega, \varphi, \theta) \otimes \mathbf{d}_3(\omega, \theta), \quad (3)$$

where \otimes is the Kronecker product, and

$$\mathbf{d}_1(\omega, \varphi, \theta) = \begin{bmatrix} 1 e^{j\frac{\omega\delta}{c}\sin\theta\cos\varphi} \\ \dots e^{j\frac{\omega\delta}{c}(M-1)\sin\theta\cos\varphi} \end{bmatrix}^T, \quad (4)$$

$$\mathbf{d}_2(\omega, \varphi, \theta) = \begin{bmatrix} 1 e^{j\frac{\omega\delta}{c}\sin\theta\sin\varphi} \\ \dots e^{j\frac{\omega\delta}{c}(M-1)\sin\theta\sin\varphi} \end{bmatrix}^T, \quad (5)$$

$$\mathbf{d}_3(\omega, \theta) = \begin{bmatrix} 1 e^{j\frac{\omega\delta}{c}\cos\theta} \\ \dots e^{j\frac{\omega\delta}{c}(M-1)\cos\theta} \end{bmatrix}^T, \quad (6)$$

are vectors of length M . In the rest of this paper, in order to simplify the notation, we drop the dependence on the angular frequency, ω . Also, we consider the first microphone, whose position is \mathbf{p}_{111} , to be the reference.

Suppose that the desired signal propagates from the direction $\{\varphi_d, \theta_d\}$. Then, the observed signal vector of length M^3 of the cube array can be expressed in the frequency domain as

$$\begin{aligned} \mathbf{y} &= \mathbf{x} + \mathbf{v} \\ &= \mathbf{d}(\varphi_d, \theta_d) X + \mathbf{v}, \end{aligned} \quad (7)$$

where X is the zero-mean desired source signal and \mathbf{v} is the zero-mean additive noise signal vector. We deduce that the covariance matrix of \mathbf{y} is

$$\begin{aligned} \Phi_{\mathbf{y}} &= E(\mathbf{y}\mathbf{y}^H) \\ &= \phi_X \mathbf{d}(\varphi_d, \theta_d) \mathbf{d}^H(\varphi_d, \theta_d) + \Phi_{\mathbf{v}} \\ &= \phi_X \mathbf{d}(\varphi_d, \theta_d) \mathbf{d}^H(\varphi_d, \theta_d) + \phi_{V_1} \Gamma_{\mathbf{v}}, \end{aligned} \quad (8)$$

where $E(\cdot)$ denotes mathematical expectation, the superscript H is the conjugate-transpose operator, $\phi_X \Delta E(|X|^2)$ is the variance of X , $\Phi_{\mathbf{v}}$ is the covariance matrix of \mathbf{v} , $\phi_{V_1} \Delta E(|V_1|^2)$ is the variance of the noise at the first (reference) sensor, and $\Gamma_{\mathbf{v}} \Delta \Phi_{\mathbf{v}} / \phi_{V_1}$ is the pseudo-coherence matrix of the noise.

With the above signal model, our objective in this paper is to study different kinds of fixed beamformers by exploiting the symmetry of the cube array.

III. CONVENTIONAL BEAMFORMING AND PERFORMANCE MEASURES

The conventional way of doing linear beamforming with a cube array is by applying a complex-valued linear filter, \mathbf{h} of length M^3 , to the observed signal vector, \mathbf{y} , i.e.,

$$Z = \mathbf{h}^H \mathbf{y}$$

$$= \mathbf{h}^H \mathbf{d}(\varphi_d, \theta_d) X + \mathbf{h}^H \mathbf{v}, \quad (9)$$

where Z is an estimate of the desired signal, X . In speech processing, it is desired to have X undistorted; therefore, the distortionless constraint on the filter is expressed as

$$\mathbf{h}^H \mathbf{d}(\varphi_d, \theta_d) = 1. \quad (10)$$

This means that the value of the beamformer pattern should be equal to 1 at $\varphi = \varphi_d$ and $\theta = \theta_d$, and smaller than (or at most equal to) 1 for $\varphi \neq \varphi_d$ and/or $\theta \neq \theta_d$. We deduce that the variance of Z is

$$\begin{aligned} \phi_Z &= \mathbf{h}^H \Phi_{\mathbf{v}} \mathbf{h} \\ &= \phi_X \left| \mathbf{h}^H \mathbf{d}(\varphi_d, \theta_d) \right|^2 + \mathbf{h}^H \Phi_{\mathbf{v}} \mathbf{h}. \end{aligned} \quad (11)$$

Next, we describe some performance measures and show how to derive some examples of optimal fixed beamformers from these measures.

A very useful measure is the beampattern; it describes the sensitivity of the beamformer to a plane wave impinging on the cube array from the direction $\{\varphi, \theta\}$. Mathematically, it is defined as [1], [17], [36]–[38]

$$\mathcal{B}(\mathbf{h}, \varphi, \theta) = \mathbf{d}^H(\varphi, \theta) \mathbf{h}. \quad (12)$$

Considering the first sensor as the reference, we see from (8) that the input signal-to-noise ratio (SNR) with respect to this reference can be defined as

$$\text{iSNR} = \frac{\phi_X}{\phi_{V_1}}. \quad (13)$$

From (11), it is clear that the output SNR is

$$\begin{aligned} \text{oSNR}(\mathbf{h}) &= \phi_X \frac{\left| \mathbf{h}^H \mathbf{d}(\varphi_d, \theta_d) \right|^2}{\mathbf{h}^H \Phi_{\mathbf{v}} \mathbf{h}} \\ &= \frac{\phi_X}{\phi_{V_1}} \times \frac{\left| \mathbf{h}^H \mathbf{d}(\varphi_d, \theta_d) \right|^2}{\mathbf{h}^H \Gamma_{\mathbf{v}} \mathbf{h}}. \end{aligned} \quad (14)$$

The definition of the SNR gain is easily derived from the two previous definitions of the input and output SNRs, i.e.,

$$\begin{aligned} \mathcal{G}(\mathbf{h}) &= \frac{\text{oSNR}(\mathbf{h})}{\text{iSNR}} \\ &= \frac{\left| \mathbf{h}^H \mathbf{d}(\varphi_d, \theta_d) \right|^2}{\mathbf{h}^H \Gamma_{\mathbf{v}} \mathbf{h}}. \end{aligned} \quad (15)$$

The most convenient way to evaluate the sensitivity of the cube array to some of its imperfections and other uncertainties is via the so-called WNG [17], [36], which is defined by taking $\Gamma_{\mathbf{v}} = \mathbf{I}_{M^3}$ in (15), where \mathbf{I}_{M^3} is the $M^3 \times M^3$ identity matrix, i.e.,

$$\mathcal{W}(\mathbf{h}) = \frac{\left| \mathbf{h}^H \mathbf{d}(\varphi_d, \theta_d) \right|^2}{\mathbf{h}^H \mathbf{h}}. \quad (16)$$

The WNG is, obviously, the SNR gain in the presence of spatially white noise. Using the Cauchy-Schwarz inequality, i.e.,

$$\left| \mathbf{h}^H \mathbf{d}(\varphi_d, \theta_d) \right|^2 \leq \mathbf{h}^H \mathbf{h} \times \mathbf{d}^H(\varphi_d, \theta_d) \mathbf{d}(\varphi_d, \theta_d), \quad (17)$$

we easily deduce from (16) that

$$\mathcal{W}(\mathbf{h}) \leq M^3, \quad \forall \mathbf{h}. \quad (18)$$

As a result, the maximum WNG is

$$\mathcal{W}_{\max} = M^3, \quad (19)$$

which is frequency and direction independent. The classical delay-and-sum or MWNG beamformer:

$$\mathbf{h}_{\text{MWNG}} = \frac{\mathbf{d}(\varphi_d, \theta_d)}{M^3}, \quad (20)$$

maximizes the WNG and, obviously, $\mathcal{W}(\mathbf{h}_{\text{MWNG}}) = \mathcal{W}_{\max}$.

Another important measure, which quantifies how directive is the beampattern, is the DF [36], [39], which is defined as

$$\begin{aligned} \mathcal{D}(\mathbf{h}) &= \frac{\left| \mathcal{B}(\mathbf{h}, \varphi_d, \theta_d) \right|^2}{\frac{1}{4\pi} \int_0^{2\pi} \int_0^\pi \left| \mathcal{B}(\mathbf{h}, \varphi, \theta) \right|^2 \sin \theta d\varphi d\theta} \\ &= \frac{\left| \mathbf{h}^H \mathbf{d}(\varphi_d, \theta_d) \right|^2}{\mathbf{h}^H \Gamma_{\mathbf{h}} \mathbf{h}}, \end{aligned} \quad (21)$$

where

$$\Gamma = \frac{1}{4\pi} \int_0^{2\pi} \int_0^\pi \mathbf{d}(\varphi, \theta) \mathbf{d}^H(\varphi, \theta) \sin \theta d\varphi d\theta. \quad (22)$$

As seen, the DF is equivalent to the SNR gain in the spherically isotropic noise field. It is clear that

$$\mathcal{D}(\mathbf{h}) \leq \mathbf{d}^H(\varphi_d, \theta_d) \Gamma^{-1} \mathbf{d}(\varphi_d, \theta_d), \quad \forall \mathbf{h}. \quad (23)$$

As a result, the maximum DF is

$$\mathcal{D}_{\max} = \mathbf{d}^H(\varphi_d, \theta_d) \Gamma^{-1} \mathbf{d}(\varphi_d, \theta_d), \quad (24)$$

which is frequency and direction dependent. Maximizing the DF, we obtain the MDF beamformer:

$$\mathbf{h}_{\text{MDF}} = \frac{\Gamma^{-1} \mathbf{d}(\varphi_d, \theta_d)}{\mathbf{d}^H(\varphi_d, \theta_d) \Gamma^{-1} \mathbf{d}(\varphi_d, \theta_d)}. \quad (25)$$

Obviously, we have $\mathcal{D}(\mathbf{h}_{\text{MDF}}) = \mathcal{D}_{\max}$.

Before ending this section, let us briefly discuss null-steering (NS) beamformers. Assume that we have an interference source in the direction $\{\varphi_0, \theta_0\} \neq \{\varphi_d, \theta_d\}$. We would like to completely cancel this interference with the beamformer \mathbf{h} and, meanwhile, fully recover the desired source coming from the direction $\{\varphi_d, \theta_d\}$. Combining these two constraints together, we get the constraint equation:

$$\mathbf{C}^H \mathbf{h} = \begin{bmatrix} 1 \\ 0 \end{bmatrix}, \quad (26)$$

where

$$\mathbf{C} = [\mathbf{d}(\varphi_d, \theta_d) \quad \mathbf{d}(\varphi_0, \theta_0)] \quad (27)$$

is the constraint matrix of size $M^3 \times 2$ whose 2 columns are linearly independent. Then, two different NS beamformers can be derived depending on what we optimize. The first one is obtained by maximizing the WNG and by taking (26) into account we get

$$\mathbf{h}_{\text{NS-MWNG}} = \mathbf{C} (\mathbf{C}^H \mathbf{C})^{-1} \begin{bmatrix} 1 \\ 0 \end{bmatrix}. \quad (28)$$

The second NS beamformer is obtained by maximizing the DF and by taking (26) into account we get

$$\mathbf{h}_{\text{NS-MDF}} = \Gamma^{-1} \mathbf{C} (\mathbf{C}^H \Gamma^{-1} \mathbf{C})^{-1} \begin{bmatrix} 1 \\ 0 \end{bmatrix}. \quad (29)$$

The beamformer $\mathbf{h}_{\text{NS-MWNG}}$ will be more robust to white noise amplification than the beamformer $\mathbf{h}_{\text{NS-MDF}}$, but the latter will be more directional than the former.

IV. FULLY SEPARABLE BEAMFORMERS

In this section, we are interested in beamformers that are fully separable, i.e.,

$$\bar{\mathbf{h}} = \mathbf{h}_1 \otimes \mathbf{h}_2 \otimes \mathbf{h}_3, \quad (30)$$

where \mathbf{h}_1 , \mathbf{h}_2 , and \mathbf{h}_3 are three complex-valued linear filters of length M . We see that we only have 3 M parameters to determine instead of M^3 in the conventional approach.

With the beamformer $\bar{\mathbf{h}}$, the beampattern is

$$\begin{aligned} \mathcal{B}(\bar{\mathbf{h}}, \varphi, \theta) &= \mathbf{d}^H(\varphi, \theta) \bar{\mathbf{h}} \\ &= [\mathbf{d}_1(\varphi, \theta) \otimes \mathbf{d}_2(\varphi, \theta) \otimes \mathbf{d}_3(\theta)]^H (\mathbf{h}_1 \otimes \mathbf{h}_2 \otimes \mathbf{h}_3) \\ &= [\mathbf{d}_1^H(\varphi, \theta) \mathbf{h}_1] [\mathbf{d}_2^H(\varphi, \theta) \mathbf{h}_2] [\mathbf{d}_3^H(\theta) \mathbf{h}_3] \\ &= \mathcal{B}_1(\mathbf{h}_1, \varphi, \theta) \times \mathcal{B}_2(\mathbf{h}_2, \varphi, \theta) \times \mathcal{B}_3(\mathbf{h}_3, \theta). \end{aligned} \quad (31)$$

We observe that the beampattern of $\bar{\mathbf{h}}$ is the product of the beampatterns of the three filters \mathbf{h}_1 , \mathbf{h}_2 , and \mathbf{h}_3 . Also, the distortionless constraint is

$$\begin{aligned} \bar{\mathbf{h}}^H \mathbf{d}(\varphi_d, \theta_d) &= 1 \\ &= \mathbf{h}_1^H \mathbf{d}_1(\varphi_d, \theta_d) \times \mathbf{h}_2^H \mathbf{d}_2(\varphi_d, \theta_d) \times \mathbf{h}_3^H \mathbf{d}_3(\theta_d). \end{aligned} \quad (32)$$

Therefore, if the individual filters are distortionless, i.e.,

$$\mathbf{h}_1^H \mathbf{d}_1(\varphi_d, \theta_d) = \mathbf{h}_2^H \mathbf{d}_2(\varphi_d, \theta_d) = \mathbf{h}_3^H \mathbf{d}_3(\theta_d) = 1, \quad (33)$$

the original beamformer $\bar{\mathbf{h}}$ is also distortionless.

In the same way, the WNG of $\bar{\mathbf{h}}$, which can also be factorized, is

$$\begin{aligned} \mathcal{W}(\bar{\mathbf{h}}) &= \frac{|\bar{\mathbf{h}}^H \mathbf{d}(\varphi_d, \theta_d)|^2}{\bar{\mathbf{h}}^H \bar{\mathbf{h}}} \\ &= \frac{|\mathbf{h}_1^H \mathbf{d}_1(\varphi_d, \theta_d)|^2}{\mathbf{h}_1^H \mathbf{h}_1} \times \frac{|\mathbf{h}_2^H \mathbf{d}_2(\varphi_d, \theta_d)|^2}{\mathbf{h}_2^H \mathbf{h}_2} \times \frac{|\mathbf{h}_3^H \mathbf{d}_3(\theta_d)|^2}{\mathbf{h}_3^H \mathbf{h}_3} \\ &= \mathcal{W}_1(\mathbf{h}_1) \times \mathcal{W}_2(\mathbf{h}_2) \times \mathcal{W}_3(\mathbf{h}_3). \end{aligned} \quad (34)$$

However, the DF of $\bar{\mathbf{h}}$ cannot be factorized in general, i.e.,

$$\begin{aligned} \mathcal{D}(\bar{\mathbf{h}}) &= \frac{|\bar{\mathbf{h}}^H \mathbf{d}(\varphi_d, \theta_d)|^2}{\bar{\mathbf{h}}^H \Gamma \bar{\mathbf{h}}} \\ &\neq \mathcal{D}_1(\mathbf{h}_1) \times \mathcal{D}_2(\mathbf{h}_2) \times \mathcal{D}_3(\mathbf{h}_3), \end{aligned} \quad (35)$$

where

$$\mathcal{D}_1(\mathbf{h}_1) = \frac{|\mathbf{h}_1^H \mathbf{d}_1(\varphi_d, \theta_d)|^2}{\mathbf{h}_1^H \Gamma_1 \mathbf{h}_1}, \quad (36)$$

$$\mathcal{D}_2(\mathbf{h}_2) = \frac{|\mathbf{h}_2^H \mathbf{d}_2(\varphi_d, \theta_d)|^2}{\mathbf{h}_2^H \Gamma_2 \mathbf{h}_2}, \quad (37)$$

$$\mathcal{D}_3(\mathbf{h}_3) = \frac{|\mathbf{h}_3^H \mathbf{d}_3(\theta_d)|^2}{\mathbf{h}_3^H \Gamma_3 \mathbf{h}_3}, \quad (38)$$

with

$$\Gamma_1 = \frac{1}{4\pi} \int_0^{2\pi} \int_0^\pi \mathbf{d}_1(\varphi, \theta) \mathbf{d}_1^H(\varphi, \theta) \sin \theta d\varphi d\theta, \quad (39)$$

$$\Gamma_2 = \frac{1}{4\pi} \int_0^{2\pi} \int_0^\pi \mathbf{d}_2(\varphi, \theta) \mathbf{d}_2^H(\varphi, \theta) \sin \theta d\varphi d\theta, \quad (40)$$

$$\Gamma_3 = \frac{1}{2} \int_0^\pi \mathbf{d}_3(\theta) \mathbf{d}_3^H(\theta) \sin \theta d\theta. \quad (41)$$

One can verify that

$$\bar{\mathbf{h}} = \mathbf{h}_1 \otimes \mathbf{h}_2 \otimes \mathbf{h}_3 = (\mathbf{I}_M \otimes \mathbf{h}_2 \otimes \mathbf{h}_3) \mathbf{h}_1 \quad (42)$$

$$= (\mathbf{h}_1 \otimes \mathbf{I}_M \otimes \mathbf{h}_3) \mathbf{h}_2 \quad (43)$$

$$= (\mathbf{h}_1 \otimes \mathbf{h}_2 \otimes \mathbf{I}_M) \mathbf{h}_3, \quad (44)$$

where \mathbf{I}_M is the $M \times M$ identity matrix. Therefore, when \mathbf{h}_2 and \mathbf{h}_3 are fixed and distortionless, we write the DF as

$$\mathcal{D}(\mathbf{h}_1 | \mathbf{h}_2, \mathbf{h}_3) = \frac{|\mathbf{h}_1^H \mathbf{d}_1(\varphi_d, \theta_d)|^2}{\mathbf{h}_1^H \Gamma_{\mathbf{h}_2, \mathbf{h}_3} \mathbf{h}_1}, \quad (45)$$

where

$$\Gamma_{\mathbf{h}_2, \mathbf{h}_3} = (\mathbf{I}_M \otimes \mathbf{h}_2 \otimes \mathbf{h}_3)^H \Gamma (\mathbf{I}_M \otimes \mathbf{h}_2 \otimes \mathbf{h}_3). \quad (46)$$

When \mathbf{h}_1 and \mathbf{h}_3 are fixed and distortionless, we write the DF as

$$\mathcal{D}(\mathbf{h}_2 | \mathbf{h}_1, \mathbf{h}_3) = \frac{|\mathbf{h}_2^H \mathbf{d}_2(\varphi_d, \theta_d)|^2}{\mathbf{h}_2^H \Gamma_{\mathbf{h}_1, \mathbf{h}_3} \mathbf{h}_2}, \quad (47)$$

where

$$\Gamma_{\mathbf{h}_1, \mathbf{h}_3} = (\mathbf{h}_1 \otimes \mathbf{I}_M \otimes \mathbf{h}_3)^H \Gamma (\mathbf{h}_1 \otimes \mathbf{I}_M \otimes \mathbf{h}_3). \quad (48)$$

In the same way, when \mathbf{h}_1 and \mathbf{h}_2 are fixed and distortionless, we write the DF as

$$\mathcal{D}(\mathbf{h}_3 | \mathbf{h}_1, \mathbf{h}_2) = \frac{|\mathbf{h}_3^H \mathbf{d}_3(\theta_d)|^2}{\mathbf{h}_3^H \Gamma_{\mathbf{h}_1, \mathbf{h}_2} \mathbf{h}_3}, \quad (49)$$

where

$$\Gamma_{\mathbf{h}_1, \mathbf{h}_2} = (\mathbf{h}_1 \otimes \mathbf{h}_2 \otimes \mathbf{I}_M)^H \Gamma (\mathbf{h}_1 \otimes \mathbf{h}_2 \otimes \mathbf{I}_M). \quad (50)$$

A. Maximum WNG

Given the structure of the WNG of $\bar{\mathbf{h}}$, it is clear that the maximization of this gain is equivalent to maximizing $\mathcal{W}_1(\mathbf{h}_1)$, $\mathcal{W}_2(\mathbf{h}_2)$, and $\mathcal{W}_3(\mathbf{h}_3)$, separately. Taking into account the distortionless constraints, we easily get the MWNG beamforming filters:

$$\mathbf{h}_{1, \text{MWNG}} = \frac{\mathbf{d}_1(\varphi_d, \theta_d)}{M}, \quad (51)$$

$$\mathbf{h}_{2, \text{MWNG}} = \frac{\mathbf{d}_2(\varphi_d, \theta_d)}{M}, \quad (52)$$

$$\mathbf{h}_{3, \text{MWNG}} = \frac{\mathbf{d}_3(\theta_d)}{M}. \quad (53)$$

As a consequence, the Kronecker product MWNG beamformer corresponding to the cube array is

$$\begin{aligned} \bar{\mathbf{h}}_{\text{MWNG}} &= \mathbf{h}_{1, \text{MWNG}} \otimes \mathbf{h}_{2, \text{MWNG}} \otimes \mathbf{h}_{3, \text{MWNG}} \\ &= \frac{\mathbf{d}_1(\varphi_d, \theta_d) \otimes \mathbf{d}_2(\varphi_d, \theta_d) \otimes \mathbf{d}_3(\theta_d)}{M^3} \\ &= \frac{\mathbf{d}(\varphi_d, \theta_d)}{M^3} = \mathbf{h}_{\text{MWNG}}, \end{aligned} \quad (54)$$

which is, of course, the classical MWNG beamformer derived in the previous section. Here, however, it is shown how the structure of the steering vector is exploited. In other words, the MWNG beamformer is determined by 3 M different coefficients only while the number of sensors is equal to M^3 .

B. Approximate Maximum DF

We can approximately maximize the DF of $\bar{\mathbf{h}}$ by maximizing the individual DFs, $\mathcal{D}_1(\mathbf{h}_1)$, $\mathcal{D}_2(\mathbf{h}_2)$, and $\mathcal{D}_3(\mathbf{h}_3)$, separately. We get

$$\mathbf{h}_{1,\text{aMDF}} = \frac{\mathbf{\Gamma}_1^{-1} \mathbf{d}_1(\varphi_d, \theta_d)}{\mathbf{d}_1^H(\varphi_d, \theta_d) \mathbf{\Gamma}_1^{-1} \mathbf{d}_1(\varphi_d, \theta_d)}, \quad (55)$$

$$\mathbf{h}_{2,\text{aMDF}} = \frac{\mathbf{\Gamma}_2^{-1} \mathbf{d}_2(\varphi_d, \theta_d)}{\mathbf{d}_2^H(\varphi_d, \theta_d) \mathbf{\Gamma}_2^{-1} \mathbf{d}_2(\varphi_d, \theta_d)}, \quad (56)$$

$$\mathbf{h}_{3,\text{aMDF}} = \frac{\mathbf{\Gamma}_3^{-1} \mathbf{d}_3(\theta_d)}{\mathbf{d}_3^H(\theta_d) \mathbf{\Gamma}_3^{-1} \mathbf{d}_3(\theta_d)}. \quad (57)$$

We deduce that the Kronecker product approximate MDF beamformer is

$$\bar{\mathbf{h}}_{\text{aMDF}} = \mathbf{h}_{1,\text{aMDF}} \otimes \mathbf{h}_{2,\text{aMDF}} \otimes \mathbf{h}_{3,\text{aMDF}}. \quad (58)$$

If we want to compromise between WNG and DF, we may want to mix the different MWNG and MDF sub-beamforming filters. Some examples are given below:

$$\bar{\mathbf{h}}_{\text{aMDF/MWNG},1} = \mathbf{h}_{1,\text{MWNG}} \otimes \mathbf{h}_{2,\text{MWNG}} \otimes \mathbf{h}_{3,\text{aMDF}}, \quad (59)$$

$$\bar{\mathbf{h}}_{\text{aMDF/MWNG},2} = \mathbf{h}_{1,\text{MWNG}} \otimes \mathbf{h}_{2,\text{aMDF}} \otimes \mathbf{h}_{3,\text{MWNG}}, \quad (60)$$

$$\bar{\mathbf{h}}_{\text{aMDF/MWNG},3} = \mathbf{h}_{1,\text{aMDF}} \otimes \mathbf{h}_{2,\text{MWNG}} \otimes \mathbf{h}_{3,\text{aMDF}}, \quad (61)$$

$$\bar{\mathbf{h}}_{\text{aMDF/MWNG},4} = \mathbf{h}_{1,\text{aMDF}} \otimes \mathbf{h}_{2,\text{aMDF}} \otimes \mathbf{h}_{3,\text{MWNG}}. \quad (62)$$

C. Null Steering

Now, let us assume that we want to place a null with multiplicity 2 in the direction $\{\varphi_0, \theta_0\} \neq \{\varphi_d, \theta_d\}$. Then, the constraints on the two filters \mathbf{h}_1 and \mathbf{h}_2 are

$$\mathbf{C}_1^H \mathbf{h}_1 = \mathbf{C}_2^H \mathbf{h}_2 = \begin{bmatrix} 1 \\ 0 \end{bmatrix}, \quad (63)$$

where

$$\mathbf{C}_1 = [\mathbf{d}_1(\varphi_d, \theta_d) \quad \mathbf{d}_1(\varphi_0, \theta_0)], \quad (64)$$

$$\mathbf{C}_2 = [\mathbf{d}_2(\varphi_d, \theta_d) \quad \mathbf{d}_2(\varphi_0, \theta_0)], \quad (65)$$

are the constraint matrices of size $M \times 2$. The maximization of the individual DFs leads to

$$\mathbf{h}_{1,\text{NS-MDF}} = \mathbf{\Gamma}_1^{-1} \mathbf{C}_1 (\mathbf{C}_1^H \mathbf{\Gamma}_1^{-1} \mathbf{C}_1)^{-1} \begin{bmatrix} 1 \\ 0 \end{bmatrix}, \quad (66)$$

$$\mathbf{h}_{2,\text{NS-MDF}} = \mathbf{\Gamma}_2^{-1} \mathbf{C}_2 (\mathbf{C}_2^H \mathbf{\Gamma}_2^{-1} \mathbf{C}_2)^{-1} \begin{bmatrix} 1 \\ 0 \end{bmatrix}. \quad (67)$$

The maximization of the individual WNGs leads to

$$\mathbf{h}_{1,\text{NS-MWNG}} = \mathbf{C}_1 (\mathbf{C}_1^H \mathbf{C}_1)^{-1} \begin{bmatrix} 1 \\ 0 \end{bmatrix}, \quad (68)$$

$$\mathbf{h}_{2,\text{NS-MWNG}} = \mathbf{C}_2 (\mathbf{C}_2^H \mathbf{C}_2)^{-1} \begin{bmatrix} 1 \\ 0 \end{bmatrix}. \quad (69)$$

As a result, two possible fully separable Kronecker product NS beamformers, which are somewhat robust to white noise amplification, are

$$\bar{\mathbf{h}}_{\text{NS},1} = \mathbf{h}_{1,\text{NS-MWNG}} \otimes \mathbf{h}_{2,\text{NS-MDF}} \otimes \mathbf{h}_{3,\text{MWNG}}, \quad (70)$$

$$\bar{\mathbf{h}}_{\text{NS},2} = \mathbf{h}_{1,\text{NS-MDF}} \otimes \mathbf{h}_{2,\text{NS-MDF}} \otimes \mathbf{h}_{3,\text{MWNG}}. \quad (71)$$

For comparison, we also give some examples that form a null with multiplicity 1:

$$\bar{\mathbf{h}}_{\text{NS},3} = \mathbf{h}_{1,\text{NS-MWNG}} \otimes \mathbf{h}_{2,\text{MWNG}} \otimes \mathbf{h}_{3,\text{MWNG}}, \quad (72)$$

$$\bar{\mathbf{h}}_{\text{NS},4} = \mathbf{h}_{1,\text{NS-MDF}} \otimes \mathbf{h}_{2,\text{MWNG}} \otimes \mathbf{h}_{3,\text{MWNG}}. \quad (73)$$

Of course, many other options are possible.

D. Iterative Maximum DF

It is always possible to fully maximize the DF in (35). For that, we need to develop an iterative algorithm. At iteration 0, we may take

$$\mathbf{h}_2^{(0)} = \mathbf{h}_{2,\text{aMDF}} \quad (74)$$

and

$$\mathbf{h}_3^{(0)} = \mathbf{h}_{3,\text{aMDF}}. \quad (75)$$

Substituting $\mathbf{h}_2^{(0)}$ and $\mathbf{h}_3^{(0)}$ into (46), we get

$$\mathbf{\Gamma}_{\mathbf{h}_{2,3}^{(0)}} = (\mathbf{I}_M \otimes \mathbf{h}_2^{(0)} \otimes \mathbf{h}_3^{(0)})^H \mathbf{\Gamma} (\mathbf{I}_M \otimes \mathbf{h}_2^{(0)} \otimes \mathbf{h}_3^{(0)}). \quad (76)$$

Now, substituting this expression into the DF in (45), we obtain at iteration 1:

$$\mathcal{D}(\mathbf{h}_1^{(1)} | \mathbf{h}_2^{(0)}, \mathbf{h}_3^{(0)}) = \frac{\left| (\mathbf{h}_1^{(1)})^H \mathbf{d}_1(\varphi_d, \theta_d) \right|^2}{(\mathbf{h}_1^{(1)})^H \mathbf{\Gamma}_{\mathbf{h}_{2,3}^{(0)}} \mathbf{h}_1^{(1)}}. \quad (77)$$

The maximization of $\mathcal{D}(\mathbf{h}_1^{(1)} | \mathbf{h}_2^{(0)}, \mathbf{h}_3^{(0)})$ with respect to $\mathbf{h}_1^{(1)}$ gives

$$\mathbf{h}_1^{(1)} = \frac{\mathbf{\Gamma}_{\mathbf{h}_{2,3}^{(0)}}^{-1} \mathbf{d}_1(\varphi_d, \theta_d)}{\mathbf{d}_1^H(\varphi_d, \theta_d) \mathbf{\Gamma}_{\mathbf{h}_{2,3}^{(0)}}^{-1} \mathbf{d}_1(\varphi_d, \theta_d)}. \quad (78)$$

Using $\mathbf{h}_1^{(1)}$ and $\mathbf{h}_3^{(0)}$ in (48), we get

$$\mathbf{\Gamma}_{\mathbf{h}_{1,3}^{(1)}} = (\mathbf{h}_1^{(1)} \otimes \mathbf{I}_M \otimes \mathbf{h}_3^{(0)})^H \mathbf{\Gamma} (\mathbf{h}_1^{(1)} \otimes \mathbf{I}_M \otimes \mathbf{h}_3^{(0)}). \quad (79)$$

As a consequence, the DF in (47) is

$$\mathcal{D}(\mathbf{h}_2^{(1)} | \mathbf{h}_1^{(1)}, \mathbf{h}_3^{(0)}) = \frac{\left| (\mathbf{h}_2^{(1)})^H \mathbf{d}_2(\varphi_d, \theta_d) \right|^2}{(\mathbf{h}_2^{(1)})^H \mathbf{\Gamma}_{\mathbf{h}_{1,3}^{(1)}} \mathbf{h}_2^{(1)}}, \quad (80)$$

whose maximization with respect to $\mathbf{h}_2^{(1)}$ gives

$$\mathbf{h}_2^{(1)} = \frac{\mathbf{\Gamma}_{\mathbf{h}_{1,3}^{(1)}}^{-1} \mathbf{d}_2(\varphi_d, \theta_d)}{\mathbf{d}_2^H(\varphi_d, \theta_d) \mathbf{\Gamma}_{\mathbf{h}_{1,3}^{(1)}}^{-1} \mathbf{d}_2(\varphi_d, \theta_d)}. \quad (81)$$

Finally, the substitution of $\mathbf{h}_1^{(1)}$ and $\mathbf{h}_2^{(1)}$ into (50) leads to

$$\mathbf{\Gamma}_{\mathbf{h}_{1,2}^{(1)}} = (\mathbf{h}_1^{(1)} \otimes \mathbf{h}_2^{(1)} \otimes \mathbf{I}_M)^H \mathbf{\Gamma} (\mathbf{h}_1^{(1)} \otimes \mathbf{h}_2^{(1)} \otimes \mathbf{I}_M), \quad (82)$$

then to the DF in (49):

$$\mathcal{D}(\mathbf{h}_3^{(1)} | \mathbf{h}_1^{(1)}, \mathbf{h}_2^{(1)}) = \frac{\left| (\mathbf{h}_3^{(1)})^H \mathbf{d}_3(\theta_d) \right|^2}{(\mathbf{h}_3^{(1)})^H \mathbf{\Gamma}_{\mathbf{h}_{1,2}^{(1)}} \mathbf{h}_3^{(1)}}, \quad (83)$$

and whose maximization gives

$$\mathbf{h}_3^{(1)} = \frac{\Gamma_{\mathbf{h}_{1,2}}^{-1} \mathbf{d}_3(\theta_d)}{\mathbf{d}_3^H(\theta_d) \Gamma_{\mathbf{h}_{1,2}}^{-1} \mathbf{d}_3(\theta_d)}. \quad (84)$$

Continuing the iterations up to the iteration n , we easily get for the first filter:

$$\mathbf{h}_1^{(n)} = \frac{\Gamma_{\mathbf{h}_{2,3}}^{-1} \mathbf{d}_1(\varphi_d, \theta_d)}{\mathbf{d}_1^H(\varphi_d, \theta_d) \Gamma_{\mathbf{h}_{2,3}}^{-1} \mathbf{d}_1(\varphi_d, \theta_d)}, \quad (85)$$

with

$$\Gamma_{\mathbf{h}_{2,3}}^{(n-1)} = \left(\mathbf{I}_M \otimes \mathbf{h}_2^{(n-1)} \otimes \mathbf{h}_3^{(n-1)} \right)^H \Gamma \left(\mathbf{I}_M \otimes \mathbf{h}_2^{(n-1)} \otimes \mathbf{h}_3^{(n-1)} \right), \quad (86)$$

for the second filter:

$$\mathbf{h}_2^{(n)} = \frac{\Gamma_{\mathbf{h}_{1,3}}^{-1} \mathbf{d}_2(\varphi_d, \theta_d)}{\mathbf{d}_2^H(\varphi_d, \theta_d) \Gamma_{\mathbf{h}_{1,3}}^{-1} \mathbf{d}_2(\varphi_d, \theta_d)}, \quad (87)$$

with

$$\Gamma_{\mathbf{h}_{1,3}}^{(n)} = \left(\mathbf{h}_1^{(n)} \otimes \mathbf{I}_M \otimes \mathbf{h}_3^{(n-1)} \right)^H \Gamma \left(\mathbf{h}_1^{(n)} \otimes \mathbf{I}_M \otimes \mathbf{h}_3^{(n-1)} \right), \quad (88)$$

and for the third filter:

$$\mathbf{h}_3^{(n)} = \frac{\Gamma_{\mathbf{h}_{1,2}}^{-1} \mathbf{d}_3(\theta_d)}{\mathbf{d}_3^H(\theta_d) \Gamma_{\mathbf{h}_{1,2}}^{-1} \mathbf{d}_3(\theta_d)}, \quad (89)$$

with

$$\Gamma_{\mathbf{h}_{1,2}}^{(n)} = \left(\mathbf{h}_1^{(n)} \otimes \mathbf{h}_2^{(n)} \otimes \mathbf{I}_M \right)^H \Gamma \left(\mathbf{h}_1^{(n)} \otimes \mathbf{h}_2^{(n)} \otimes \mathbf{I}_M \right). \quad (90)$$

Therefore, the fully separable Kronecker product iterative MDF beamformer is at iteration n :

$$\tilde{\mathbf{h}}_{\text{MDF}}^{(n)} = \mathbf{h}_1^{(n)} \otimes \mathbf{h}_2^{(n)} \otimes \mathbf{h}_3^{(n)}. \quad (91)$$

V. PARTIALLY SEPARABLE BEAMFORMERS

In this section, we study beamformers that are only partially separable, i.e.,

$$\tilde{\mathbf{h}} = \mathbf{h}_{12} \otimes \mathbf{h}_3, \quad (92)$$

where \mathbf{h}_{12} and \mathbf{h}_3 are two complex-valued linear filters of lengths M^2 and M , respectively. The illustration of the partially Kronecker product decomposition is shown in Fig. 2. We see that we have $M^2 + M$ parameters to determine and $3M \leq M^2 + M < M^3$ (for $M \geq 2$).

With the beamformer $\tilde{\mathbf{h}}$, the beampattern can be decomposed as

$$\begin{aligned} \mathcal{B}(\tilde{\mathbf{h}}, \varphi, \theta) &= [\mathbf{d}_{12}(\varphi, \theta) \otimes \mathbf{d}_3(\theta)]^H (\mathbf{h}_{12} \otimes \mathbf{h}_3) \\ &= [\mathbf{d}_{12}^H(\varphi, \theta) \mathbf{h}_{12}] [\mathbf{d}_3^H(\theta) \mathbf{h}_3] \\ &= \mathcal{B}_{12}(\mathbf{h}_{12}, \varphi, \theta) \times \mathcal{B}_3(\mathbf{h}_3, \theta), \end{aligned} \quad (93)$$

where $\mathbf{d}_{12}(\varphi, \theta) = \mathbf{d}_1(\varphi, \theta) \otimes \mathbf{d}_2(\varphi, \theta)$.

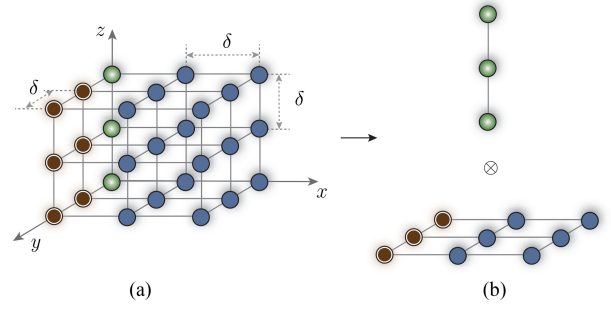


Fig. 2. Illustration of the Kronecker product decomposition of a cube array into a uniform planar subarray and a uniform linear subarray: (a) the cube array and (b) the decomposed planar and linear subarrays.

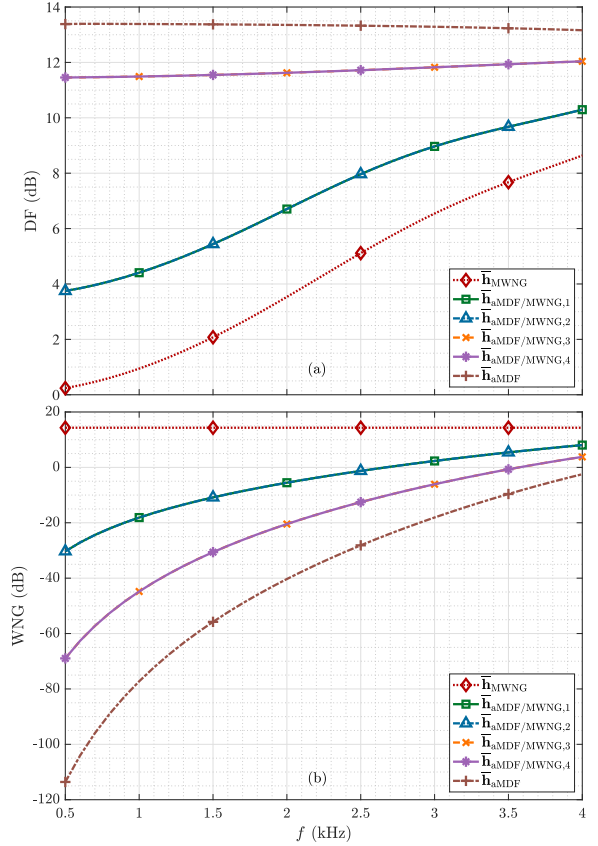


Fig. 3. WNGs and DFs of the fully separable Kronecker product MWNG beamformer, Kronecker product approximate MDF beamformer, and beamformers compromising between DF and WNG as a function of frequency, f , with a cube microphone array: (a) WNGs and (b) DFs. Conditions of simulations: $M = 3$, $\delta = 2.2$ cm, and $\{\varphi_d, \theta_d\} = \{0^\circ, 90^\circ\}$. Note that the same curve with different marks indicates that two curves coincide exactly.

We can also decompose the WNG as follows:

$$\begin{aligned} \mathcal{W}(\tilde{\mathbf{h}}) &= \frac{|\mathbf{h}_{12}^H \mathbf{d}_{12}(\varphi_d, \theta_d)|^2}{\mathbf{h}_{12}^H \mathbf{h}_{12}} \times \frac{|\mathbf{h}_3^H \mathbf{d}_3(\theta_d)|^2}{\mathbf{h}_3^H \mathbf{h}_3} \\ &= \mathcal{W}_{12}(\mathbf{h}_{12}) \times \mathcal{W}_3(\mathbf{h}_3). \end{aligned} \quad (94)$$

The DF of $\tilde{\mathbf{h}}$, however, cannot be factorized in general, i.e.,

$$\mathcal{D}(\tilde{\mathbf{h}}) = \frac{|\tilde{\mathbf{h}}^H \mathbf{d}(\varphi_d, \theta_d)|^2}{\tilde{\mathbf{h}}^H \Gamma \tilde{\mathbf{h}}}$$

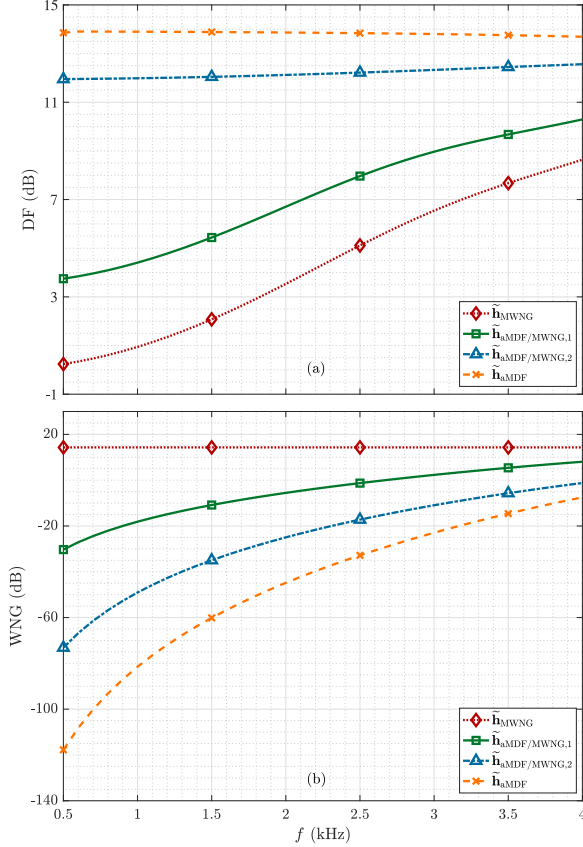


Fig. 4. WNGs and DFs of the partially separable Kronecker product MWNG beamformer, Kronecker product approximate MDF beamformer, and beamformers compromising between DF and WNG as a function of frequency, f , with a cube microphone array: (a) WNGs and (b) DFs. Conditions of simulations: $M = 3$, $\delta = 2.2$ cm, and $\{\varphi_d, \theta_d\} = \{0^\circ, 90^\circ\}$.

$$\neq \mathcal{D}_{12}(\mathbf{h}_{12}) \times \mathcal{D}_3(\mathbf{h}_3), \quad (95)$$

where

$$\mathcal{D}_{12}(\mathbf{h}_{12}) = \frac{|\mathbf{h}_{12}^H \mathbf{d}_{12}(\varphi_d, \theta_d)|^2}{\mathbf{h}_{12}^H \mathbf{\Gamma}_{12} \mathbf{h}_{12}}, \quad (96)$$

$$\mathcal{D}_3(\mathbf{h}_3) = \frac{|\mathbf{h}_3^H \mathbf{d}_3(\theta_d)|^2}{\mathbf{h}_3^H \mathbf{\Gamma}_3 \mathbf{h}_3}, \quad (97)$$

with

$$\mathbf{\Gamma}_{12} = \frac{1}{4\pi} \int_0^{2\pi} \int_0^\pi \mathbf{d}_{12}(\varphi, \theta) \mathbf{d}_{12}^H(\varphi, \theta) \sin \theta d\varphi d\theta, \quad (98)$$

$$\mathbf{\Gamma}_3 = \frac{1}{2} \int_0^\pi \mathbf{d}_3(\theta) \mathbf{d}_3^H(\theta) \sin \theta d\theta. \quad (99)$$

One can verify that

$$\tilde{\mathbf{h}} = \mathbf{h}_{12} \otimes \mathbf{h}_3 = (\mathbf{I}_{M^2} \otimes \mathbf{h}_3) \mathbf{h}_{12} \quad (100)$$

$$= (\mathbf{h}_{12} \otimes \mathbf{I}_M) \mathbf{h}_3, \quad (101)$$

where \mathbf{I}_{M^2} is the $M^2 \times M^2$ identity matrix. Therefore, when \mathbf{h}_3 is fixed and distortionless, we write the DF as

$$\mathcal{D}(\mathbf{h}_{12}|\mathbf{h}_3) = \frac{|\mathbf{h}_{12}^H \mathbf{d}_{12}(\varphi_d, \theta_d)|^2}{\mathbf{h}_{12}^H \mathbf{\Gamma}_{\mathbf{h}_3} \mathbf{h}_{12}}, \quad (102)$$

where

$$\mathbf{\Gamma}_{\mathbf{h}_3} = (\mathbf{I}_{M^2} \otimes \mathbf{h}_3)^H \mathbf{\Gamma} (\mathbf{I}_{M^2} \otimes \mathbf{h}_3). \quad (103)$$

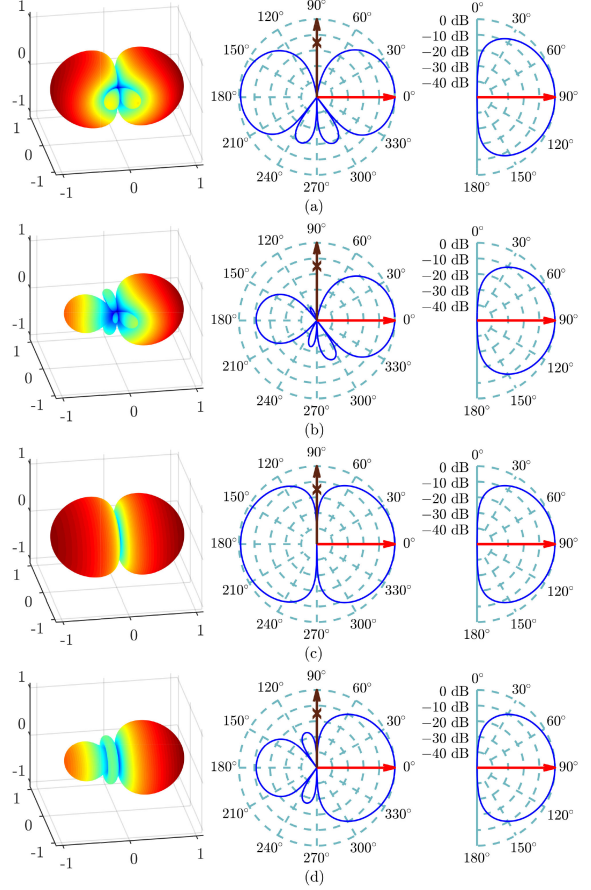


Fig. 5. Beampatterns of the fully separable Kronecker product NS beamformers with a cube microphone array: (a) $\tilde{\mathbf{h}}_{\text{NS},1}$, (b) $\tilde{\mathbf{h}}_{\text{NS},2}$, (c) $\tilde{\mathbf{h}}_{\text{NS},3}$, and (d) $\tilde{\mathbf{h}}_{\text{NS},4}$. The left subplots show the three-dimensional beampattern, the center subplots show the two-dimensional beampattern for $\theta = 90^\circ$, and the right subplots show the two-dimensional beampattern for $\varphi = 0^\circ$. Conditions of simulations: $M = 3$, $\delta = 2.2$ cm, $f = 2$ kHz, $\{\varphi_d, \theta_d\} = \{0^\circ, 90^\circ\}$, and $\{\varphi_0, \theta_0\} = \{90^\circ, 90^\circ\}$.

Also, when \mathbf{h}_{12} is fixed and distortionless, we write the DF as

$$\mathcal{D}(\mathbf{h}_3|\mathbf{h}_{12}) = \frac{|\mathbf{h}_3^H \mathbf{d}_3(\varphi_d, \theta_d)|^2}{\mathbf{h}_3^H \mathbf{\Gamma}_{\mathbf{h}_{12}} \mathbf{h}_3}, \quad (104)$$

where

$$\mathbf{\Gamma}_{\mathbf{h}_{12}} = (\mathbf{h}_{12} \otimes \mathbf{I}_M)^H \mathbf{\Gamma} (\mathbf{h}_{12} \otimes \mathbf{I}_M). \quad (105)$$

Now, we have all the tools and measures to derive different kinds of fixed beamformers in the same way we did in the previous section, which will not be presented for conciseness.

VI. SIMULATIONS

In this section, we study the performance of the proposed Kronecker product beamformers through simulations. We consider a cube array with $M = 3$, so the number of microphones is $3 \times 3 \times 3 = 27$. The interelement spacing is chosen as $\delta = 2.2$ cm, and the desired direction is set as $\{\varphi_d, \theta_d\} = \{0^\circ, 90^\circ\}$.

We first discuss a group of Kronecker product beamformers including the Kronecker product MWNG beamformers, the Kronecker product approximate MDF beamformers, and beamformers compromising between WNG and DF for the case of

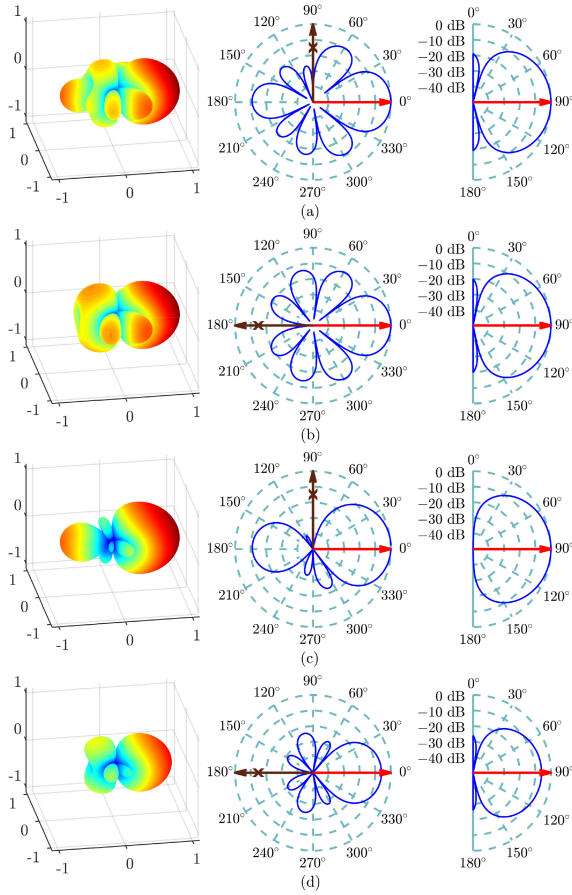


Fig. 6. Beam patterns of the partially separable Kronecker product NS beamformers with a cube microphone array for different beamformers and φ_0 : (a) \bar{h}_{NS} , $\varphi_0 = 90^\circ$, (b) $\varphi_0 = 180^\circ$. (c) $\bar{h}_{NS,2}$, $\varphi_0 = 90^\circ$, and (d) $\bar{h}_{NS,2}$, $\varphi_0 = 180^\circ$. The left subplots show the three-dimensional beam pattern, the center subplots show the two-dimensional beam pattern for $\theta = 90^\circ$, and the right subplots show the two-dimensional beam pattern for $\varphi = 0^\circ$. Conditions of simulations: $M = 3$, $\delta = 2.2$ cm, $f = 2$ kHz, $\{\varphi_d, \theta_d\} = \{0^\circ, 90^\circ\}$, and $\theta_0 = 90^\circ$.

full separation. Figure 3 shows plots of the WNG and the DF of the beamformers: \bar{h}_{MWNG} , $\bar{h}_{aMDF/MWNG,1}$, $\bar{h}_{aMDF/MWNG,2}$, $\bar{h}_{aMDF/MWNG,3}$, $\bar{h}_{aMDF/MWNG,4}$, and \bar{h}_{aMDF} , as a function of frequency, f . It is easily seen that the Kronecker product approximate MDF beamformer achieves the highest level of DF but it has the smallest value of WNG. Conversely, the Kronecker product MWNG beamformer obtains the highest level of WNG but it has the smallest value of DF. One can see that the beamformers $\bar{h}_{aMDF/MWNG,1}$ and $\bar{h}_{aMDF/MWNG,2}$ have the same values of WNG and DF at each frequency. The same happens between the beamformers $\bar{h}_{aMDF/MWNG,3}$ and $\bar{h}_{aMDF/MWNG,4}$. This result is understandable as the three subarrays are identical excepts their directions.

The second set of simulations investigates the impact of the decomposition on the performance of the beamformer. Figure 4 shows plots of the DF and WNG of the same group of Kronecker product beamformers as in the previous simulation but for the case of partial separation. Comparing with the results in Fig. 3, one can see that the Kronecker product MWNG beamformer for both decompositions obtains the same result, which corroborates

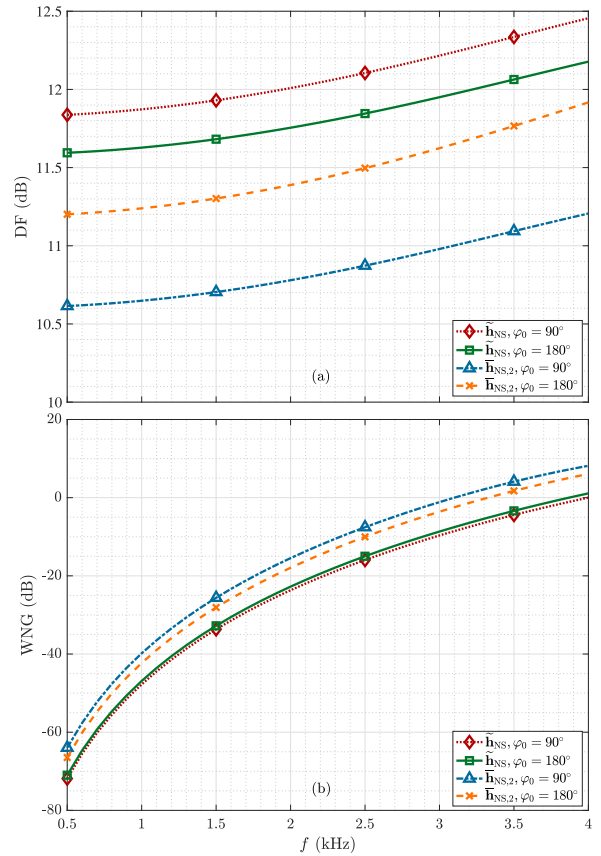


Fig. 7. WNGs and DFs of the partially separable Kronecker product NS beamformers as a function of frequency, f , with a cube microphone array for different beamformers and φ_0 : (a) WNGs and (b) DFs. Conditions of simulations: $M = 3$, $\delta = 2.2$ cm, $\{\varphi_d, \theta_d\} = \{0^\circ, 90^\circ\}$, and $\theta_0 = 90^\circ$.

with the theoretical analysis that the Kronecker product MWNG beamformers for both decompositions are equivalent to the conventional MWNG beamformer. We can also see that the Kronecker product approximate MDF beamformer with partial separation achieves a higher value of DF than the fully separable Kronecker product approximate MDF beamformer, but at the expense that more coefficients need to be determined.

Next, we study the Kronecker product NS beamformer for the case of full separation. We mainly discuss four of them, i.e., the beamformers $\bar{h}_{NS,1}$, $\bar{h}_{NS,2}$, $\bar{h}_{NS,3}$, and $\bar{h}_{NS,4}$, where the first two beamformers form a null with multiplicity of 2 and the last two beamformers form a null with multiplicity of 1. We consider the case of $\{\varphi_0, \theta_0\} = \{90^\circ, 90^\circ\}$. Figure 5 plots the beam patterns of these beamformers at frequency $f = 2$ kHz, where the left subplots show the three-dimensional beam pattern, the central subplots show the two-dimensional beam pattern for $\theta = 90^\circ$, and the right subplots show the two-dimensional beam pattern for $\varphi = 0^\circ$. As expected, the beamformers $\bar{h}_{NS,1}$ and $\bar{h}_{NS,2}$ have deeper and wider nulls than the beamformers $\bar{h}_{NS,3}$ and $\bar{h}_{NS,4}$, which are able to suppress more effectively the interference incident from the null directions. This shows the superiority on designing NS beamformers with nulls of several multiplicities by the Kronecker product beamforming.

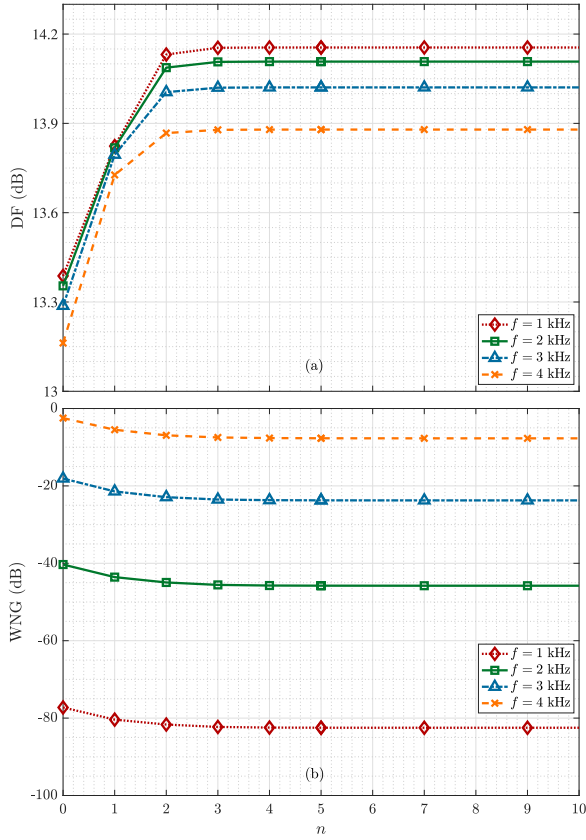


Fig. 8. WNGs and DFs of the fully separable Kronecker product MDF beamformer as a function of iteration times, n , with a cube microphone array for different frequencies, f : (a) WNGs and (b) DFs. Conditions of simulations: $M = 3$, $\delta = 2.2$ cm, and $\{\varphi_d, \theta_d\} = \{0^\circ, 90^\circ\}$.

Now, let us compare the performances of the Kronecker product NS beamformers between the fully separable and partially separable cases. We mainly concentrate on the fully separable Kronecker product NS beamformer $\bar{\mathbf{h}}_{\text{NS},2}$ and the partially separable Kronecker product NS beamformer $\tilde{\mathbf{h}}_{\text{NS}}$. In this simulation, the angle θ_0 is set to 90° . Figure 6(a) and (b) plot the beampatterns of the beamformer $\tilde{\mathbf{h}}_{\text{NS}}$ ($\tilde{\mathbf{h}}_{\text{NS}} = \mathbf{h}_{12,\text{NS-MDF}} \otimes \mathbf{h}_{3,\text{MWNG}}$) with $\varphi_0 = 90^\circ$ and $\varphi_0 = 180^\circ$, respectively, and Fig. 6(c) and (d) plot the beampattern of the beamformer $\bar{\mathbf{h}}_{\text{NS},2}$ ($\bar{\mathbf{h}}_{\text{NS},2} = \mathbf{h}_{1,\text{NS-MDF}} \otimes \mathbf{h}_{2,\text{NS-MDF}} \otimes \mathbf{h}_{3,\text{MWNG}}$) with $\varphi_0 = 90^\circ$ and $\varphi_0 = 180^\circ$, respectively, at $f = 2$ kHz. Figure 7 shows the corresponding DFs and WNGs as a function of frequency, f . It is seen that both these two beamformers can obtain a relatively high value of DF. In comparison, for the same angle of null, the beamformer $\tilde{\mathbf{h}}_{\text{NS}}$ can achieve higher value of DF than the beamformer $\bar{\mathbf{h}}_{\text{NS},2}$ as shown in Fig. 7.

We notice from Fig. 6(d) that the gain of the beamformer $\bar{\mathbf{h}}_{\text{NS},2}$ at the look direction $\{\varphi_d, \theta_d\} = \{0^\circ, 90^\circ\}$ is not 1 so the desired signal will be distorted. The underlying reason for this is that in this special situation where $\{\varphi_d, \theta_d\} = \{0^\circ, 90^\circ\}$ and $\{\varphi_0, \theta_0\} = \{180^\circ, 90^\circ\}$, the steering vector $\mathbf{d}_2(\omega, \theta_d, \varphi_d) = \mathbf{d}_2(\omega, \theta_0, \varphi_0)$ and thus the constraint matrix $\mathbf{C}_2 = [\mathbf{d}_2(\varphi_d, \theta_d) \ \mathbf{d}_2(\varphi_0, \theta_0)]$ is not full rank. In contrast, the partially separable Kronecker product NS can better deal with this as is shown in Fig. 6(c). This is understandable as

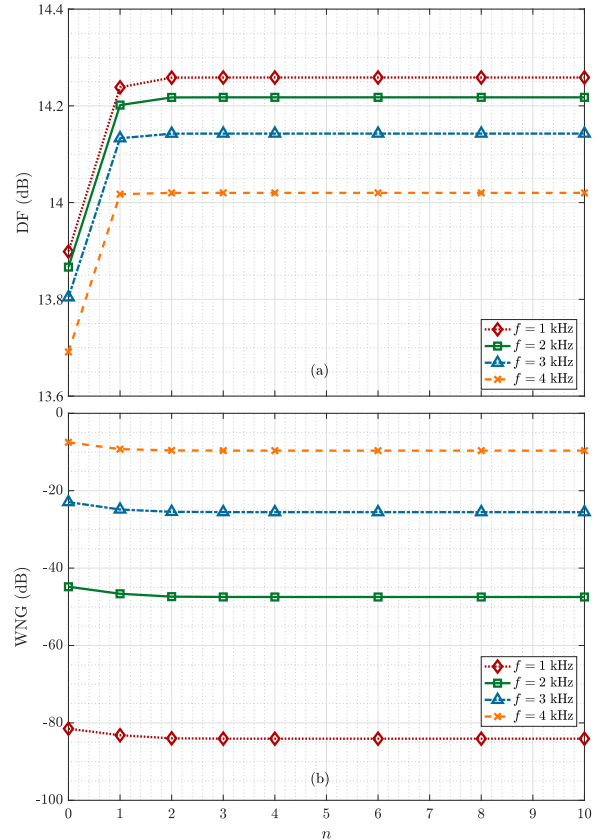


Fig. 9. WNGs and DFs of the partially separable Kronecker product MDF beamformer as a function of iteration times, n , with a cube microphone array for different frequencies $f \in \{1, 2, 3, 4\}$ kHz: (a) WNGs and (b) DFs. Conditions of simulations: $M = 3$, $\delta = 2.2$ cm, and $\{\varphi_d, \theta_d\} = \{0^\circ, 90^\circ\}$.

in the fully separable case the null is of multiplicity of 2 while in the partially separable case the null is only of multiplicity of 1.

Finally, we analyze the performance of the Kronecker product iterative MDF beamformer. Again, we start with the fully separable case. Figure 8 plots the DFs and WNGs of the fully separable Kronecker product iterative MDF beamformer as a function of the number of iterations, n , for different frequencies $f \in \{1, 2, 3, 4\}$ kHz, where the beamformer at the iteration 0 is equivalent to the fully separable Kronecker product approximate maximum DF beamformer. It is easily seen that the algorithm converges in 4 iterations. Similarly, the results for the partially separable Kronecker product iterative MDF beamformer are shown in Fig. 9. As seen, the algorithm converges in 3 iterations.

VII. CONCLUSIONS

We have investigated Kronecker product beamforming for 3D cube microphone arrays. The Kronecker product decomposition was divided into two cases: fully and partially separable ones. The former decomposes the global beamformer into the Kronecker product of three sub-beamformers corresponding to three linear subarrays, so only $3M$ coefficients are needed for designing the sub-beamformers and the global Kronecker product beamformer given M^3 sensors. The latter decomposes the global beamformer into the Kronecker product of two sub-beamformers: one corresponds to a planar subarray and the

other corresponds to a linear subarray orthogonal to the planar one. In this case, a total of $M^2 + M$ coefficients are needed for designing the sub-beamformers and the global Kronecker product beamformer. In each case, different criteria were used to design the sub-beamforming filters, resulting a number of optimal and suboptimal sub-beamformers. Through combinations of those sub-beamformers in the Kronecker product, we showed how to design different beamformers with cube microphone arrays, each having different performance properties. We also presented methods to design null-steering beamformers with the Kronecker product decomposition and an iterative algorithm to maximize the global DF. Experimental results have validated the design methods and demonstrated the properties of the different decompositions and beamformers.

REFERENCES

- [1] J. Benesty, J. Chen, and Y. Huang, *Microphone Array Signal Processing*. Berlin, Germany: Springer-Verlag, 2008, pp. 1–239.
- [2] M. Brandstein and D. Ward, *Microphone Arrays: Signal Processing Techniques and Applications*. Berlin, Germany: Springer-Verlag, 2001, pp. 1–416.
- [3] B. Rafaely, *Fundamentals of Spherical Array Processing*. Berlin, Germany: Springer-Verlag, 2015, pp. 1–201.
- [4] S. Gannot, D. Burshtein, and E. Weinstein, “Signal enhancement using beamforming and nonstationarity with applications to speech,” *IEEE Trans. Signal Process.*, vol. 49, no. 8, pp. 1614–1626, Aug. 2001.
- [5] C. Bouchard, D. I. Havelock, and M. Bouchard, “Beamforming with microphone arrays for directional sources,” *J. Acoust. Soc. Amer.*, vol. 125, no. 4, pp. 2098–2104, Apr. 2009.
- [6] S. Markovich, S. Gannot, and I. Cohen, “Multichannel eigenspace beamforming in a reverberant noisy environment with multiple interfering speech signals,” *IEEE Trans. Audio, Speech, Lang. Process.*, vol. 17, no. 6, pp. 1071–1086, Aug. 2009.
- [7] G. Huang, J. Chen, and J. Benesty, “Insights into frequency-invariant beamforming with concentric circular microphone arrays,” *IEEE/ACM Trans. Audio, Speech, Lang. Process.*, vol. 26, no. 12, pp. 2305–2318, Dec. 2018.
- [8] S. Doclo and M. Moonen, “GSVD-based optimal filtering for single and multimicrophone speech enhancement,” *IEEE Trans. Signal Process.*, vol. 50, no. 9, pp. 2230–2244, Sep. 2002.
- [9] J. R. Jensen, G.-O. Glentis, M. G. Christensen, A. Jakobsson, and S. H. Jensen, “Fast LCMV-based methods for fundamental frequency estimation,” *IEEE Trans. Signal Process.*, vol. 61, no. 12, pp. 3159–3172, Jun. 2013.
- [10] O. Schwartz, S. Gannot, and E. A. Habets, “Multispeaker LCMV beamformer and postfilter for source separation and noise reduction,” *IEEE/ACM Trans. Audio, Speech, Lang. Process.*, vol. 25, no. 5, pp. 940–951, May 2017.
- [11] H. Cox, R. M. Zeskind, and T. Kooij, “Practical supergain,” *IEEE Trans. Acoust., Speech, Signal Process.*, vol. 34, no. 3, pp. 393–398, Jun. 1986.
- [12] E. Mabande, A. Schad, and W. Kellermann, “Design of robust superdirective beamformers as a convex optimization problem,” in *Proc. IEEE Int. Conf. Acoust., Speech Signal Process.*, 2009, pp. 77–80.
- [13] S. Doclo and M. Moonen, “Superdirective beamforming robust against microphone mismatch,” *IEEE Trans. Acoust., Speech, Signal, Process.*, vol. 15, no. 2, pp. 617–631, Feb. 2007.
- [14] M. Crocco and A. Trucco, “Design of robust superdirective arrays with a tunable tradeoff between directivity and frequency-invariance,” *IEEE Trans. Signal Process.*, vol. 59, no. 5, pp. 2169–2181, May 2011.
- [15] J. Bitzer and K. U. Simmer, “Superdirective microphone arrays,” in *Microphone Arrays*, M. Brandstein and D. Ward, Eds. Berlin, Germany: Springer, 2001, ch. 2, pp. 19–38.
- [16] L. C. Parra, “Steerable frequency-invariant beamforming for arbitrary arrays,” *J. Acoust. Soc. Amer.*, vol. 119, no. 6, pp. 3839–3847, Jun. 2006.
- [17] J. Benesty and J. Chen, *Study and Design of Differential Microphone Arrays*. Berlin, Germany: Springer-Verlag, 2012, pp. 1–180.
- [18] G. Huang, J. Benesty, and J. Chen, “On the design of frequency-invariant beampatterns with uniform circular microphone arrays,” *IEEE/ACM Trans. Audio, Speech, Lang. Process.*, vol. 25, no. 5, pp. 1140–1153, May 2017.
- [19] G. W. Elko, “Differential microphone arrays,” in *Audio Signal Processing for Next-Generation Multimedia Communication Systems*, Y. Huang and J. Benesty, Eds. Berlin, Germany: Springer., 2004, ch. 2, pp. 11–65.
- [20] E. De Sena, H. Hacıhabiboglu, and Z. Cvetkovic, “On the design and implementation of higher order differential microphones,” *IEEE Trans. Audio, Speech, Lang. Process.*, vol. 20, no. 1, pp. 162–174, Jan. 2012.
- [21] G. Huang, J. Chen, and J. Benesty, “Design of planar differential microphone arrays with fractional orders,” *IEEE/ACM Trans. Audio, Speech, Lang. Process.*, vol. 28, pp. 116–130, Oct. 2020.
- [22] J. Lovatello, A. Bernardini, and A. Sarti, “Steerable circular differential microphone arrays,” in *Proc. Eur. Sig. Process. Conf.*, 2018, pp. 11–15.
- [23] H. L. Van Trees, *Optimum Array Processing: Part IV of Detection, Estimation, and Modulation Theory*. Hoboken, NJ, USA: Wiley, 2004, pp. 1–1443.
- [24] R. A. Monzingo and T. W. Miller, *Introduction to Adaptive Arrays*. Raleigh, NC, USA: SciTech., 2004, pp. 1–544.
- [25] R. Berkun, I. Cohen, and J. Benesty, “Combined beamformers for robust broadband regularized superdirective beamforming,” *IEEE/ACM Trans. Audio, Speech, Lang. Process.*, vol. 23, no. 5, pp. 877–886, May 2015.
- [26] G. Huang, J. Benesty, and J. Chen, “Superdirective beamforming based on the Krylov matrix,” *IEEE/ACM Trans. Audio, Speech, Lang. Process.*, vol. 24, no. 12, pp. 2531–2543, Dec. 2016.
- [27] J. Benesty, I. Cohen, and J. Chen, *Array Processing: Kronecker Product Beamforming*. Berlin, Germany: Springer-Verlag, 2019, pp. 1–189.
- [28] I. Cohen, J. Benesty, and J. Chen, “Differential Kronecker product beamforming,” *IEEE/ACM Trans. Audio, Speech, Lang. Process.*, vol. 27, no. 5, pp. 892–902, May 2019.
- [29] W. Yang, G. Huang, J. Benesty, I. Cohen, and J. Chen, “On the design of flexible Kronecker product beamformers with linear microphone arrays,” in *Proc. IEEE Int. Conf. Acoust., Speech Signal Process.*, 2019, pp. 441–445.
- [30] X. Wang, J. Benesty, G. Huang, J. Chen, and I. Cohen, “Design of Kronecker product beamformers with cuboid microphone arrays,” in *Proc. Int. Congr. Acoust.*, 2019, pp. 2660–2667.
- [31] G. Huang, I. Cohen, J. Benesty, and J. Chen, “Kronecker product beamforming with multiple differential microphone arrays,” in *Proc. IEEE Sensor Array Multichannel Signal Process.*, 2020, pp. 1–5.
- [32] G. Huang, J. Benesty, J. Chen, and I. Cohen, “Robust and steerable Kronecker product differential beamforming with rectangular microphone arrays,” in *Proc. IEEE Int. Conf. Acoust., Speech Signal Process.*, 2020, pp. 211–215.
- [33] X. Zhao, J. Benesty, J. Chen, and G. Huang, “Differential beamforming from the beampattern factorization perspective,” *IEEE/ACM Trans. Audio, Speech, Lang. Process.*, vol. 29, pp. 632–643, Dec. 2020.
- [34] R. Sharma, I. Cohen, and J. Benesty, “Adaptive and hybrid Kronecker product beamforming for far-field speech signals,” *Speech Commun.*, vol. 120, pp. 42–52, Jun. 2020.
- [35] G. Itzhak, J. Benesty, and I. Cohen, “On the design of differential Kronecker product beamformers,” *IEEE/ACM Trans. Audio, Speech, Lang. Process.*, vol. 29, pp. 1397–1410, Mar. 2021.
- [36] G. W. Elko and J. Meyer, “Microphone Arrays,” in *Springer Handbook of Speech Processing*, J. Benesty, M. M. Sondhi, and Y. Huang, Eds. Berlin, Germany: Springer-Verlag, 2008, ch. 48, pp. 1021–1041.
- [37] D. E. Dudgeon, “Fundamentals of digital array processing,” in *Proc. IEEE*, vol. 65, no. 6, pp. 898–904, Jun. 1977.
- [38] D. H. Johnson and D. E. Dudgeon, *Array Signal Processing: Concepts and Techniques*. London, U.K.: Pearson, 1993, pp. 111–198.
- [39] L. L. Beranek, *Acoustics*. Woodbury, NY, USA: Acoustical Society of America, 1986, pp. 91–109.



Xuehan Wang received the bachelor’s degree in electronics and information engineering from the Northwestern Polytechnical University, Xi’an, China, in 2016. She is currently working toward the Ph.D. degree with the Center of Immersive and Intelligent Acoustics, Northwestern Polytechnical University, and also a Visiting Ph.D. Student with the Department of Electrical Engineering, Technion–Israel Institute of Technology, Haifa, Israel. Her research interests include speech enhancement, audio signal processing, and microphone array signal processing.



Jacob Benesty received the master's degree in microwaves from Pierre and Marie Curie University, Paris, France, in 1987, and the Ph.D. degree in control and signal processing from Orsay University, Orsay, France, in April 1991. During the Ph.D. degree from November 1989 to April 1991, he worked on adaptive filters and fast algorithms with Centre National d'Etudes des Telecommunications, Paris, France. From 1994 to 1995, he was with Telecom Paris University, Paris, France, on multichannel adaptive filters and acoustic echo cancellation. From 1995

to 2003, he was first a Consultant and then a Member of the Technical Staff with Bell Laboratories, Murray Hill, NJ, USA. In May 2003, he joined the University of Quebec, INRS-EMT, Montreal, QC, Canada, as a Professor. He is also an Adjunct Professor with Aalborg University, Denmark, a Guest Professor with Northwestern Polytechnical University, Xi'an, China, and a Visiting Professor with the Technion, Haifa, Israel.

In particular, he was the Lead Researcher with Bell Labs who conceived and designed the world-first real-time hands-free full-duplex stereophonic teleconferencing system. He also conceived and designed the world-first PC-based multiparty hands-free full-duplex stereo conferencing system over IP networks. He has coauthored and coedited or coauthored numerous books in the area of acoustic signal processing. His research interests include signal processing, acoustic signal processing, and multimedia communications. He is the inventor of many important technologies. He is the Editor of the book series *Springer Topics in Signal Processing*. He was the General Chair and Technical Chair of many international conferences and a Member of various IEEE technical committees. Four of his journal papers were awarded by the IEEE Signal processing Society and in 2010 he was the recipient of the Gheorghe Cartianu Award from the Romanian Academy.



Jingdong Chen received the Ph.D. degree in pattern recognition and intelligence control from the Chinese Academy of Sciences, Beijing, China, in 1998.

From 1998 to 1999, he was with ATR Interpreting Telecommunications Research Laboratories, Kyoto, Japan, where he conducted research on speech synthesis, speech analysis, and objective measurements for evaluating speech synthesis. He then joined the Griffith University, Brisbane, QLD, Australia, where he engaged in research on robust speech recognition and signal processing. From 2000 to 2001, he was

with ATR Spoken Language Translation Research Laboratories on robust speech recognition and speech enhancement. From 2001 to 2009, he was a Member of Technical Staff with Bell Laboratories, Murray Hill, NJ, USA, working on acoustic signal processing for telecommunications. He subsequently joined WeVoice Inc., Bridgewater Township, NJ, USA, as the Chief Scientist. He is currently a Professor with Northwestern Polytechnical University, Xi'an, China. He co-authored 12 monograph books including *Array Processing—Kronecker Product Beamforming*, (Springer, 2019), *Fundamentals of Signal Enhancement and Array Signal Processing*, (Wiley, 2018), *Fundamentals of Differential Beamforming*, (Springer, 2016), *Design of Circular Differential Microphone Arrays* (Springer, 2015), *Noise Reduction in Speech Processing* (Springer, 2009), *Microphone Array Signal Processing* (Springer, 2008), and *Acoustic MIMO Signal Processing* (Springer, 2006). His research interests include array signal processing, adaptive signal processing, speech enhancement, adaptive noise or echo control, signal separation, speech communication, and artificial intelligence.

From 2008 to 2014, he was an Associate Editor for the IEEE TRANSACTIONS ON AUDIO, SPEECH, AND LANGUAGE PROCESSING and from 2007 to 2009, a Technical Committee (TC) Member of the IEEE Signal Processing Society (SPS) TC on Audio and Electroacoustics. He is currently the Chair of IEEE Xi'an Section and a Member of the IEEE SPS TC on Audio and Acoustic Signal Processing. He was the General Co-Chair of ACM WUWNET 2018 and IWAENC 2016, the Technical Program Chair of IEEE TENCON 2013, a Technical Program Co-Chair of IEEE WASPAA 2009, IEEE ChinaSIP 2014, IEEE ICSPCC 2014, and IEEE ICSPCC 2015, and helped organize many other conferences.

He was the recipient of the 2008 Best Paper Award from the IEEE Signal Processing Society (with Benesty, Huang, and Doclo), the Best Paper Award

from the IEEE Workshop on Applications of Signal Processing to Audio and Acoustics in 2011 (with Benesty), the Bell Labs Role Model Teamwork Award twice in 2009 and 2007, respectively, the NASA Tech Brief Award twice in 2010 and 2009, respectively, and the Young Author Best Paper Award from the 5th National Conference on Man-Machine Speech Communications in 1998. He is a co-author of a paper for which C. Pan was the recipient of the IEEE R10 (Asia-Pacific Region) Distinguished Student Paper Award (First Prize) in 2016. He was also the recipient of the Japan Trust International Research Grant from the Japan Key Technology Center in 1998 and the Distinguished Young Scientists Fund from the National Natural Science Foundation of China in 2014.



Gongping Huang received the bachelor's degree in electronics and information engineering and the Ph.D. degree in information and communication engineering from the Northwestern Polytechnical University, Xian, China, in 2012 and 2019, respectively. He is currently a Postdoctoral Research Fellow with the Faculty of Electrical Engineering, Technion – Israel Institute of Technology, Haifa, Israel. From 2015 to 2017, he was a Visiting Researcher with the University of Quebec, INRS-EMT, Montreal, QC, Canada.

He has authored or coauthored more than 50 papers in highly-ranked international journals and conferences, which include IEEE/ACM TRANSACTIONS ON AUDIO, SPEECH, AND LANGUAGE PROCESSING, JOURNAL OF THE ACOUSTICAL SOCIETY OF AMERICA, and holds four U.S. Patents. His research interests include microphone arrays, acoustic signal processing, and speech enhancement. He was the recipient of the Andrew and Erna Finci Viterbi Post-Doctoral Fellowship's Award in 2019 and the Best Ph.D. Thesis Award of Chinese Institute of Electronics in 2020. He is an active Reviewer for many scientific journals and international conferences including the IEEE TRANSACTIONS ON AUDIO, SPEECH, AND LANGUAGE PROCESSING, IEEE TRANSACTIONS ON SIGNAL PROCESSING, IEEE TRANSACTIONS ON MULTIMEDIA, IEEE SIGNAL PROCESSING LETTERS, IEEE TRANSACTIONS ON VEHICULAR TECHNOLOGY, IEEE TRANSACTIONS ON MECHATRONICS, *Journal of the Acoustical Society of America*, *Speech Communication*, ICASSP, IWAENC, INTERSPEECH, and EUSIPCO.



Israel Cohen received the B.Sc. (Summa Cum Laude), M.Sc. and Ph.D. degrees in electrical engineering from the Technion–Israel Institute of Technology, Haifa, Israel, in 1990, 1993, and 1998, respectively. He is the Louis and Samuel Seidan Professor of electrical and computer engineering with the Technion–Israel Institute of Technology. He is also a Visiting Professor with Northwestern Polytechnical University, Xi'an, China.

From 1990 to 1998, he was a Research Scientist with RAFAEL Research Laboratories, Haifa, Israel, Ministry of Defense. From 1998 to 2001, he was a Postdoctoral Research Associate with Computer Science Department, Yale University, New Haven, CT, USA. In 2001, he joined the Faculty of Electrical and Computer Engineering, Technion.

His research interests include array processing, statistical signal processing, deep learning, analysis and modeling of acoustic signals, speech enhancement, noise estimation, microphone arrays, source localization, blind source separation, system identification, and adaptive filtering.

Dr. Cohen was awarded the Norman Seiden Prize for Academic Excellence in 2017, the SPS Signal Processing Letters Best Paper Award in 2014, the Alexander Goldberg Prize for Excellence in Research in 2010, and the Muriel and David Jacknow Award for Excellence in Teaching in 2009. He is the Coeditor of the Multichannel Speech Processing Section of the *Springer Handbook of Speech Processing* (Springer, 2008), and the coauthor of *Fundamentals of Signal Enhancement and Array Signal Processing* (Wiley-IEEE Press, 2018). He was an Associate Editor for the IEEE TRANSACTIONS ON AUDIO, SPEECH, AND LANGUAGE PROCESSING and IEEE SIGNAL PROCESSING LETTERS, a Member of the IEEE Audio and Acoustic Signal Processing Technical Committee and the IEEE Speech and Language Processing Technical Committee, and a Distinguished Lecturer of the IEEE Signal Processing Society.